Aggregation Effects on Single-Scattering Properties of Ice Crystals

J. Um and G.M. McFarquhar
Department of Atmospheric Sciences
University of Illinois at Urbana-Champaign
Urbana, Illinois

Introduction

Impacts of cirrus on the energy budget of the earth and their representation in climate models have been identified as important and unsolved problems (Ramanathan et al. 1983; Liou 1986). Parameterization schemes for large-scale models that describe the scattering properties of cirrus are based upon the single-scattering properties of well-defined ice crystals (e.g., column, dendrite, plate, and bullet rosette) that are not major components of cirrus in many in-situ observations. Irregularly shaped ice crystals and aggregates of ice crystals are frequently observed in-situ, but have not previously been considered in the development of parameterization schemes.

During spiral descents of the University of North Dakota Citation through cirrus of a non-convective origin over the Atmospheric Radiation Measurement program (ARM) Southern Great Plains site, aggregates of bullet rosettes (hereafter ABRs) were observed (Figure 1) at temperatures between -15 and 50°C using a Cloud Particle Imager (CPI), which has 2.3 μm resolution and was developed by Stratton Park Engineering Co. (SPEC, Inc.). Many of these ABRs consisted of clusters of two or more bullet rosettes attached together so that there was more than one point from which the component bullets emanated. Because of this, these ABRs are said to have more than one local center of mass. Here the single-scattering properties for idealized models describing these observed ABRs are computed using a ray-tracing code (Macke 1993; Macke et al. 1996) at six wavelengths.

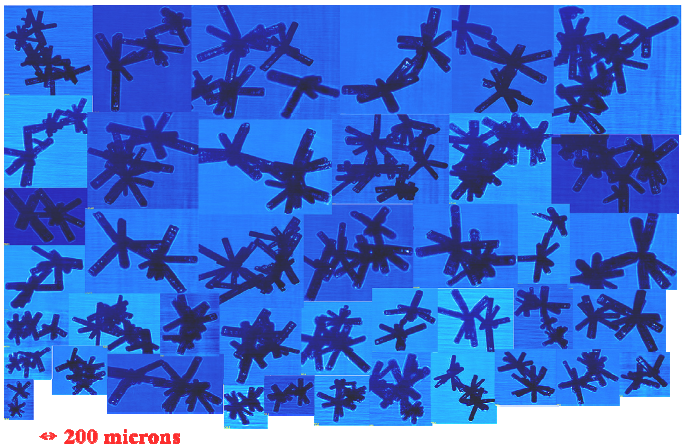

Figure 1. ABRs imaged by CPI during the 2000 Cloud IOP over ARM's SGP site.

Table 1. Geometry of fundamental element bullets.

Bullet Type	Length (L)	Radius (R)	Height (H)	Aspect Ratio (L/2R)	Tip Angle
Bullet_1	100	34.1605	55.6391	1.46	28°
Bullet_2	120	39.0325	63.5745	1.54	28°
Bullet_3	140	42.9685	69.9852	1.63	28°
Bullet_4	160	45.9685	74.8715	1.74	28°
Bullet_5	180	48.0325	78.2333	1.87	28°
Bullet_6	200	49.1605	80.0705	2.03	28°

Note: Unit of length, radius, and height is μm.

Geometric Model of Ice Crystal

Using high-resolution CPI observations of images of ABRs as guidance, the geometry of ice crystals are described by the coordinates of the vertices in a three-dimensional Cartesian coordinate system. A plane equation defining a surface consists of three points in that surface. The geometric coordinates of ABRs were determined from the conjunction of three planes, which gives the point where the two bullet rosettes attach. At this conjunction, two bullet rosettes stick together without overlap.

In this paper, six types of bullet (Table 1) are used to determine the effects of bullet aspect ratio, bullet size and aggregate shape on the single-scattering properties (i.e., phase function and asymmetry parameter). The pyramidal tip angle was assumed to be 28° regardless of the bullet type. Therefore, the relationship between the radius of columar body (R) and the pyramidal tip height (H) is given as

$$R = \frac{2\sqrt{3}H}{3\tan 62^{\circ}}. \qquad (1)$$

Henceforth, the notation y_name_x is used to describe the crystals used in the scattering computations, where y denotes the number of attached bullets or rosettes, x denotes the bullet or bullet rosette type, and name is the type of crystal considered (bullet or bullet rosette, benoted br). For the purpose of this study, a bullet rosette is assumed to consist of six bullets. For example, 3_br_2 indicates three bullet rosettes, each consisting of type 2 bullets, are attached together and 6_bullet_1 indicates that 6 type 1 bullets are attached together. The geometries of the ice crystals used in this paper are shown in Figure 2. In this paper, six types of bullet rosettes, attached together without overlap, are used to define the ABRs used for computing single-scattering properties. An example of an idealized ABRs together with CPI measurements of ABRs are shown in Figure 3. Table 2 shows the six different wavelengths and refrative indices of ice for which the single-scattering properties are computed.

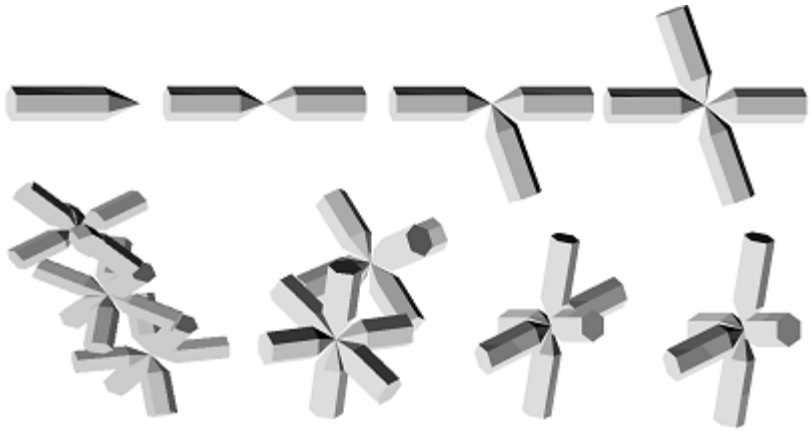

Figure 2. Idealized geometry of 1_bullet, 2_bullet, 3_bullet, 4_bullet, 5_bullet, 1_br (6_bullets), 2_br (12_bullet), and 3_br (18_bullet) from top left clockwise.

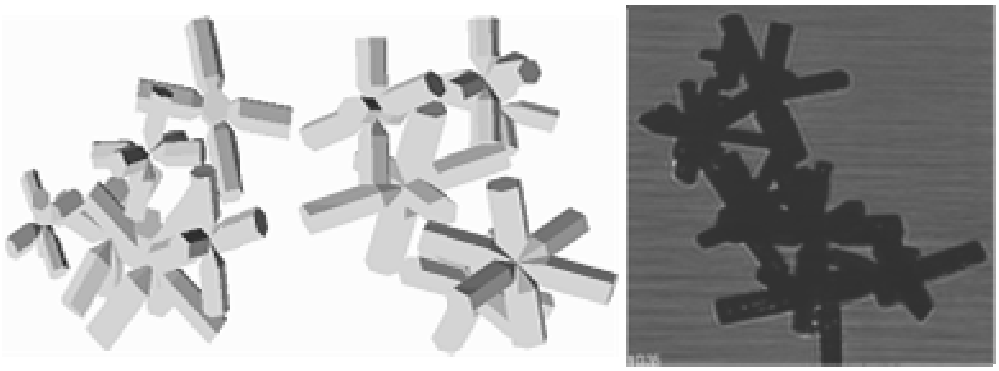

Figure 3. Idealized geometry of two ABRs (left panel) and image of ABRs observed with CPI (right panel) during the 2000 IOP.

Table 2. Wavlengths, real and imaginary part of refractive index of ice.

Wavelength	mr	Mi
0.47	1.3145	1.550 E-09
0.55	1.3110	3.110 E-09
1.24	1.2972	1.220 E-05
1.38	1.2943	1.580 E-05
1.65	1.2878	2.410 E-04
2.13	1.2674	5.650 E-04

Results

Aspect Ratio Effect

Figure 4 shows how the scattering phase function P_{11} varies with angle for the six different types of bullets used in this study. Each panel corresponds to a different wavelength. The general features noted in Figure 4 are two well-known 22° and 46° halos caused by minimum deviation at 60° and 90° for ice prisms, broad 150˚ maxima, backward scattering and an unusual 9° peak. Even though the 9° halo is unusual, it has been observed (Neiman 1989). This unusual peak is caused by refractions associated with a triangle face in pyramidal top and an opposite side rectangular face in column. The angle between the two faces is 28°.

For all six wavelengths, lateral and backward scattering (70° to 180°) decrease with bullet size. However, this lateral and backward scattering decrease is not due to increasing size, but rather due to increasing aspect ratio (aspect ratios of the six bullets are listed in Table 1). The increasing aspect ratio increases the amount of forward scattering and diminishes the lateral scattering. The decrease of the lateral scattering becomes more significant with increasing wavelength. This occurs because the imaginary part of the refractive index increases with wavelength so that absorption is more effective at longer wavelengths, and hence the lateral scattering is reduced by the absorption. Figure 5 is identical to Figure 4 except that the scattering properties are shown for bullet rosettes, instead of for bullets. The aspect ratio effect for bullet rosettes is similar to that for bullets. The only difference is that the lateral and backward scattering for bullet rosettes are bigger and smoother than for bullets. Some of the small peaks are not present for the case of bullet rosettes because the structure of a bullet rosette is more complex than that of a bullet. The more complex structure of bullet rosette allows more light to be scattered into lateral and backward scattering regions. Furthermore, due to the complex structure, internal reflections within a bullet rosette are more effective than within a bullet and photons are more likely to reenter a bullet rosette than a bullet. The photons that escape from one branch can reenter another. The number of reentering photons decreases when the aspect ratio becomes larger. Therefore, the lateral and backward scattering of the bullet rosette are bigger than those of the bullet and are reduced as aspect ratio increases.

Figure 6 summarizes the results of the scattering simulations, by showing that the asymmetry parameter increases with the aspect ratio for all six wavelengths. This is caused by more forward diffraction and less lateral scattering with increasing wavelength. It is also seen that the asymmetry parameter of a bullet rosette is smaller than that of its component bullets, even though the bullet rosette is bigger than the bullet. At 0.55 μm wavelength, the difference in asymmetry parameter between 1_bullet_1 and 1_bullet_6 is 0.024 and that between 1_br_1 and 1_br_6 is 0.03, while at 2.13 μm wavelength the differences are 0.0296 and 0.033 respectively. Since there is no size effect at a non-absorbing wavelength, these differences are solely caused by the aspect ratio effect. This means that an incorrect choice of ice crystal aspect ratio can cause more than 3% error in calculating solar radiation reaching the Earth.

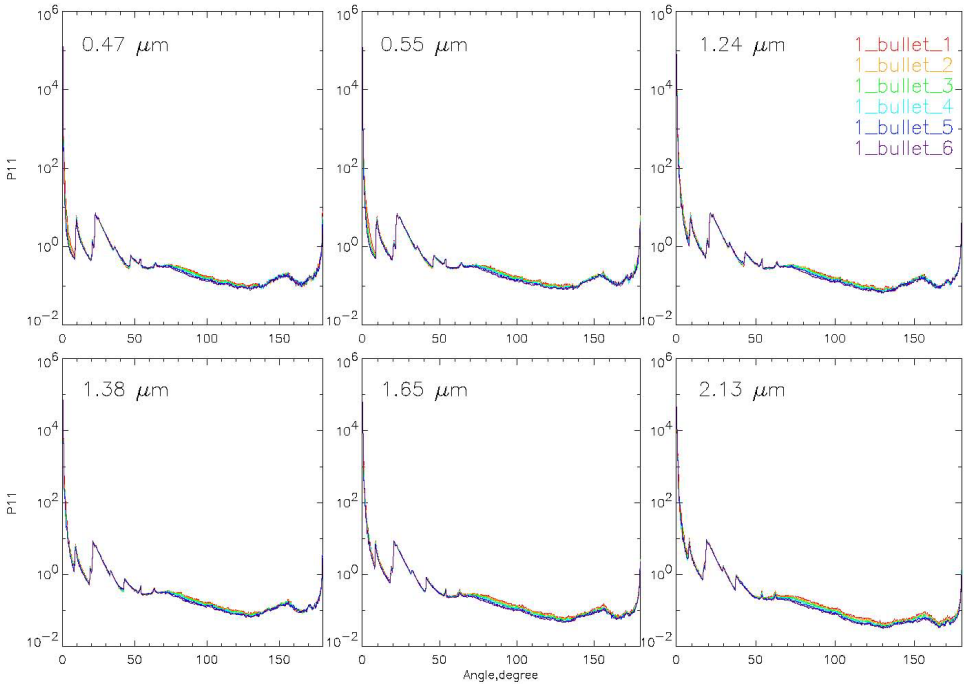

Figure 4. Phase function of six different types of bullets at six wavelengths.

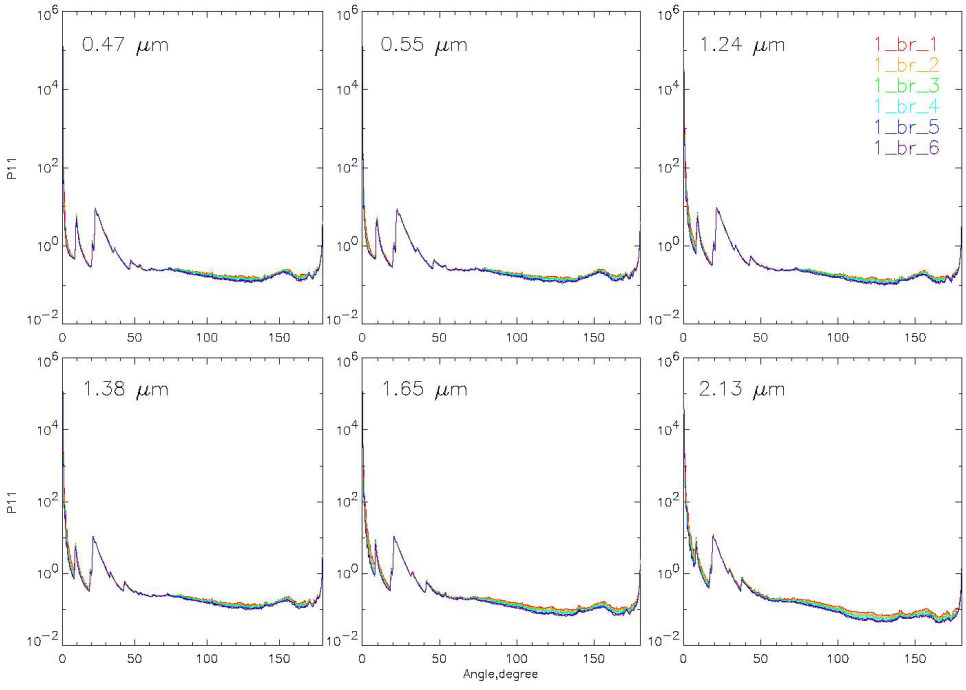

Figure 5. Phase function of six different types of bullet rosettes at six wavelengths.

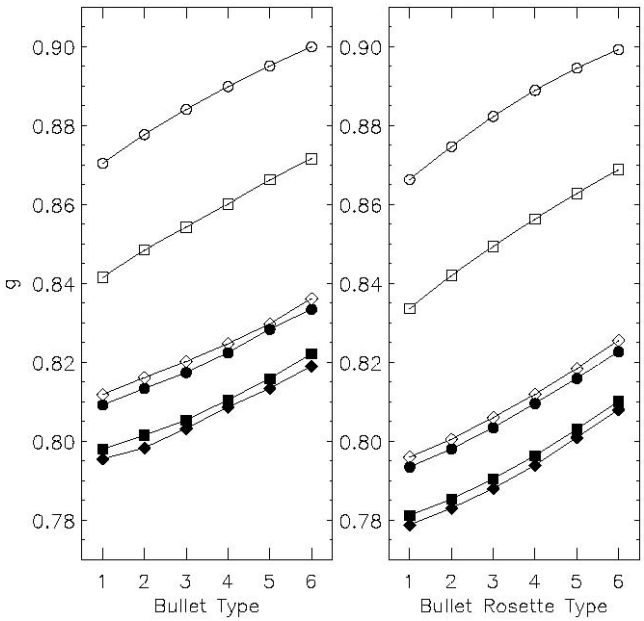

Figure 6. Asymmetry parameter of bullets (left) and bullet rosettes (right) with different bullet types at six wavelengths. 0.47, 0.55, 1.24, 1.38, 1.65, and 2.13 μm are represented by filled diamond, filled square, filled circle, diamond, square, and circle, respectively.

Aggregation Effect

Figure 7 shows how aggregation impacts the calculated asymmetry parameters. This figure shows the asymmetry parameters for 1_bullet, 2_bullet, 3_bullet, 4_bullet, 5_bullet, 1_br (6_bullet), 2_br (12_bullet), and 3_br (18 bullet) at six wavelengths. As the number of bullets or bullet rosettes attached to a crystal increases, the asymmetry parameter decreases. A more complex ice crystal structure increases the lateral scattering and hence causes the asymmetry parameter to decrease. However, this trend becomes weak at an absorbing wavelength. For example, the asymmetry parameter difference between 1_bullet_6 and 3_br_6 is less than 0.0019 at 2.13 μm wavelength. On the other hand, the difference between 1_bullet_1 and 1_bullet_6 is 0.03 at the same wavelength. This implies that the type of ice crystal is more important than the aggregation effect for determining the asymmetry parameter. It was verified that the aggregation effect reduces the asymmetry parameter with an increasing number of aggregating ice crystal components at non-absorbing wavelengths. Hence, the aggregation and absorbing effect cancel each other at absorbing wavelengths, meaning that the asymmetry parameter is almost constant.

Aggregates of Bullet Rosettes (ABRs)

ABRs may consist of several bullet rosettes. In this paper, a cluster of six different size bullet rosettes is regarded as ABRs. Figure 8 shows the nonzero elements of the scattering phase matrix at absorbing and non-absorbing wavelengths for a bullet rosette (1_br_EA) which has the equivalent project area of the ABRs shown in the plot (area difference error is less than 3%), and ABRs. The main characteristics of the phase function for the ABRs are similar to those of for the 1_br_EA, namely pronounced peaks at 9°, 22°, and relatively small peaks at 46°. However, notable differences, such as an almost one order of

magnitude difference in the direct forward scattering for all six wavelengths exist. This implies that the delta-function transmission due to ice crystal geometry with parallel plane facets is significantly diminished because of the complex structure of ABRs. The lateral scattering for the ABRs is bigger than that of 1_br_EA due to the complex structure. This occurs because light emerging from one component ice crystal can reenter another adjacent ice crystal in the complex geometry. This light undergoing several internal reflections can then be scattered into lateral and backward directions. Therefore, the lateral and backward scattering readily occur within ABRs and act to reduce the asymmetry parameter. This combination of the decrease in direct forward scattering and the increase of lateral scattering leads to a decrease in the asymmetry parameter of the ABRs.

The asymmetry parameters of ABRs and 1_br_EA at six wavelengths are shown in Figure 9. The difference in asymmetry parameter between ABRs and 1_br_EA is 0.068 and 0.043 at 0.55 and 2.13 μm wavelengths respectively. At a non-absorbing wavelength (0.55 μm), the scattering properties depend only on the ice crystal's shape or geometry. At absorbing wavelengths, the asymmetry parameters also depend on the absorbing characteristics of the ice crystal. Therefore, the ice crystal size becomes important at absorbing wavelengths. The path-length of light becomes longer for bigger ice crystals, resulting in more absorption within ice crystals.

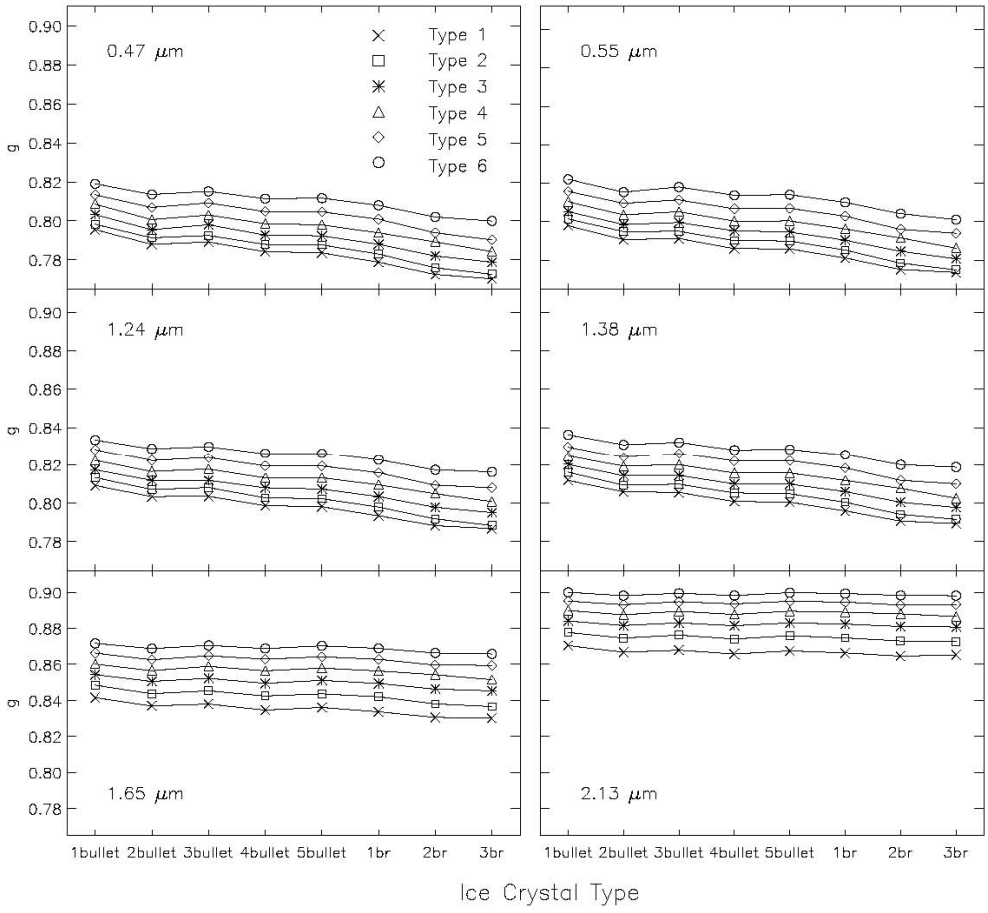

Figure 7. Variation of calculated asymmetry parameter for combinations of bullets in bullet rosettes, and combination of bullet rosettes into ABRs.

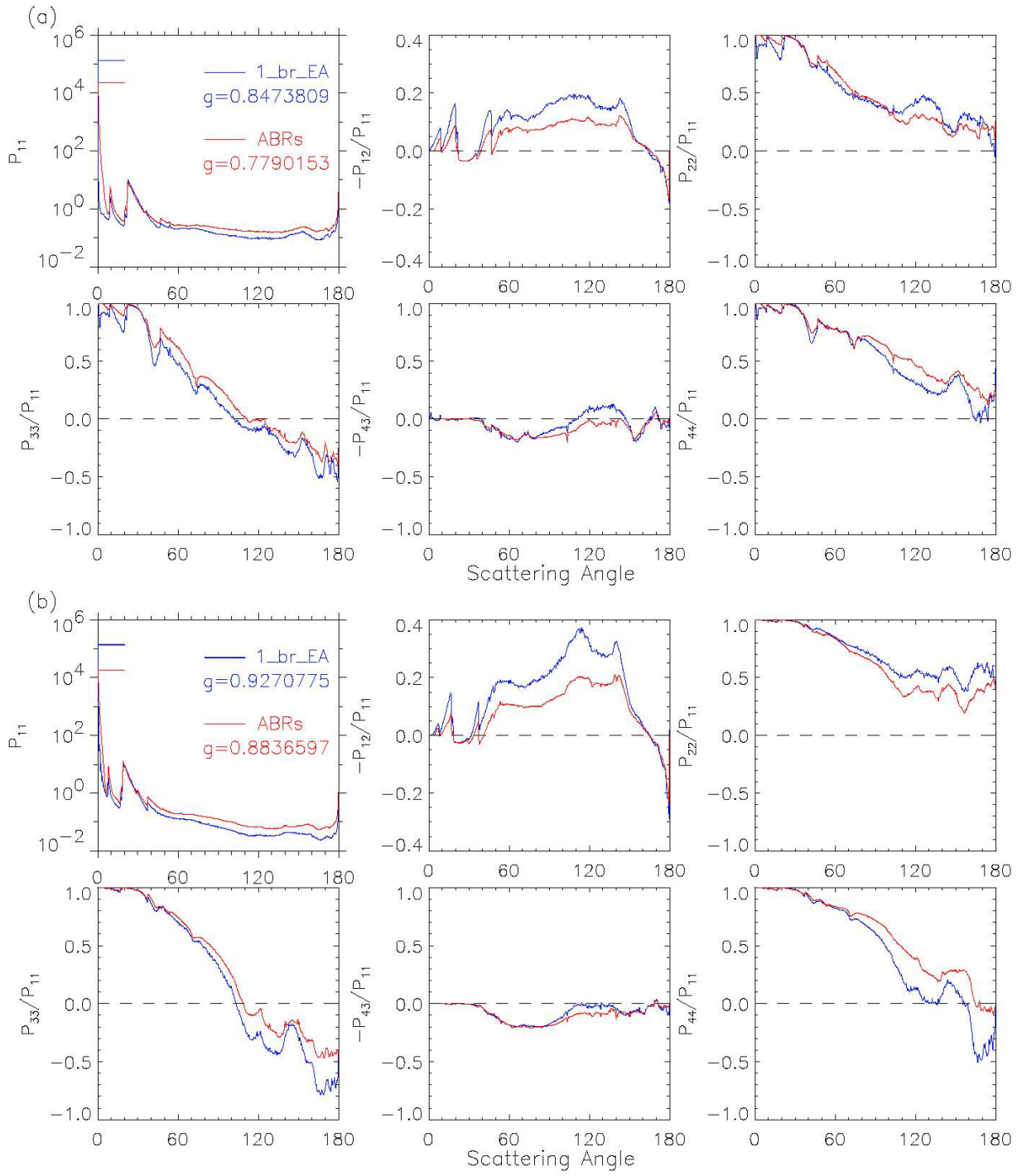

Figure 8. Asymmetry parameter and nonzero phase matrix elements for an equivalent project area bullet rosette (1_br_EA, blue) and ABRs (red) at (a) 0.55 μm and (b) 2.13 μm wavelength. The direct forward scattering is indicated by a bar at scattering angle of 0˚.

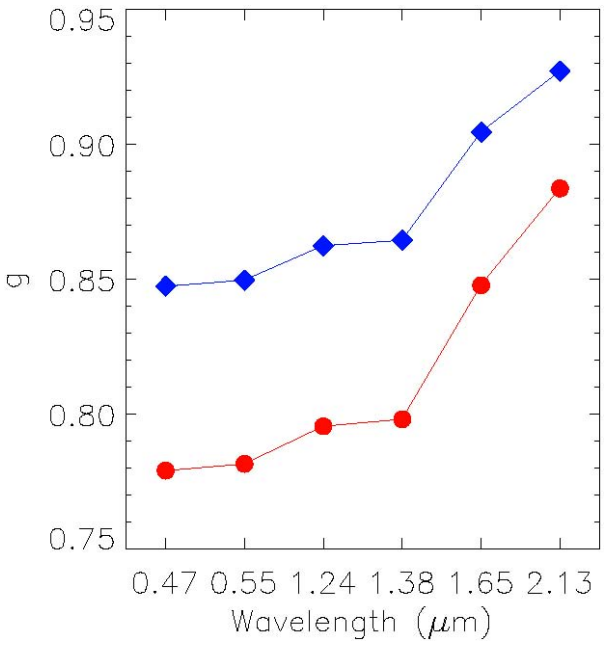

Figure 9. Asymmetry parameter of 1_br_EA (blue) and ABRs (red) at six wavelengths.

The Degree of Linear Polarization (DLP) reveals negative values associated with broad 22° peak, 46° peak and backscattering region. Both ABRs and 1_br_EA have positive P_{22}/P_{11} values for entire scattering angles at both wavelengths. Other phase matrix elements show differences as well and these provide useful information of multi-scattering within complex ice crystals for lidar measurements.

Conclusions

The single scattering properties of bullets, bullet rosettes, and ABRs were calculated using a ray-tracing method at six wavelengths. The most important results of this study are summarized as follows:

- ABRs have more lateral scattering and less forward scattering than of the other crystal types studied here and therefore a smaller asymmetry parameter (g=0.7815) than bullets (g=0.8089, average of 6 types bullets), bullet rosettes (g=0.7944, average of 6 types of bullet rosettes) and equivalent project area bullet rosette (g=0.8496) at 0.55 μm wavelength.

- g for an equivalent projected area bullet rosette differs by 8.72% from that of ABRs, a significant difference given Vogelman and Ackerman (1995) found 2 to 5% accuracy in g was required for radiative flux calculations needed for climate studies.

- When aggregates consist solely of bullet rosettes, the aggregates have a similar phase function as their components. For example, ABRs consisting of mixtures of bullet rosettes have the same well-known peaks (i.e., 9°, 22°, 46° halos) as bullet rosettes.

- As aspect ratio increases, g increases regardless of ice crystal type (bullet, bullet rosette, and ABRs). However, g decreases with the number of bullets or bullet rosettes contained in the aggregate crystal.

- At 0.55 μm wavelength the difference in g (0.024) due to variations in aspect ratio (e.g., type 1 and 6 bullet) is bigger than that (0.016) due to variations in the manner in which the component crystals are combined.

- For accurate retrieval of cirrus clouds in terms of remote sensing, a priori information about aspect ratio and habit of ice crystals is required.

Acknowledgements

This research was supported by the Department of Energy Atmospheric Radiation Measurement (ARM) program under grant DE-FG03-02ER63337. Data were obtained from the ARM program sponsored by the U.S. Department of Energy, Office of Science, Office of Biological and Environmental Research, Environmental Services Divisions. We thank Andreas Macke for providing advice and the codes used to simulate scattering.

Contact

Junshik Um, junum@atmos.uiuc.edu, (217) 333-9056

References

Liou, KN. 1986. "Review: Influence of cirrus clouds on weather and climate process: A global perspective." *Monthly Weather Review* 114, 1167-1199.

Macke, A. 1993. "Scattering of light by polyhedral ice crystals." *Applied Optics* 32, 2780-2788.

Macke, A, J Muller, and E Rasche. 1996. "Single scattering properties of atmospheric crystals." *Journal of Atmospheric Science* 53, 2813-2825.

Neiman, PJ. 1989. "The Boulder, Colorado, concentric halo display of 21 July 1986." *Bulletin of the American Meteorological Society* 70, 258-264.

Ramanathan, V, EJ Pitcher, RC Malone, and ML Blackmon. 1983. "The response of a spectral General Circulation Model to refinements in radiative processes." *Journal of Atmospheric Science* 40, 605-630.

Vogelmann, AM, and TP Ackerman. 1995. "Relating cirrus properties to observed fluxes: A critical assessment." *Journal of Atmospheric Science* 52, 4285-4301.